

162, 801 (1965) [Sov. Phys. Dokl. 10, 532 (1965)]. For a review see S. Kogan and T. M. Lifshits, Phys. Status Solidi (a) 39, 11 (1977).

<sup>2</sup>E. E. Haller and W. L. Hansen, Solid State Commun. 15, 687 (1974).

<sup>3</sup>M. S. Skolnik, L. Eaves, R. A. Stradling, T. C. Portal, and S. Askenazy, Solid State Commun. 15, 1403 (1974).

<sup>4</sup>E. E. Haller, in Proceedings of the First Seminar on Photoelectric Spectroscopy of Semiconductors, Moscow, May 1977 (to be published).

<sup>5</sup>R. C. Frank and T. C. Thomas, J. Phys. Chem. Solids 16, 144 (1960).

<sup>6</sup>R. N. Hall, in *Lattice Defects in Semiconductors 1974*, Institute of Physics Conference Series No. 23, edited by F. A. Huntley (Institute of Physics, London,

1975), p. 190.

<sup>7</sup>R. L. Jones and P. Fisher, J. Phys. Chem. Solids 26, 1125 (1965).

<sup>8</sup>R. A. Faulkner, Phys. Rev. 184, 713 (1968).

<sup>9</sup>D. K. Wilson, Phys. Rev. 134, A265 (1964).

<sup>10</sup>E. E. Haller, to be published.

<sup>11</sup>S. T. Wang and C. Kittel, Phys. Rev. B 7, 713 (1973).

<sup>12</sup>R. N. Hall and T. J. Soltys, to be published.

<sup>13</sup>E. E. Haller, G. S. Hubbard, W. L. Hansen, and A. Seeger, in *Mechanical Properties at High Rates of Strain*, Institute of Physics Conference Series No. 21, edited by J. Harding (Institute of Physics, London, 1974), p. 309.

<sup>14</sup>E. E. Haller and G. S. Hubbard, in Proceedings of the First Seminar on Photoelectric Spectroscopy of Semiconductors, Moscow, May 1977 (to be published).

## Evidence for a Ferromagnet-Spin-Glass Transition in PdFeMn

B. H. Verbeek, G. J. Nieuwenhuys, H. Stocker, and J. A. Mydosh  
*Kamerlingh Onnes Laboratorium der Rijks-Universiteit, Leiden, The Netherlands*  
 (Received 9 January 1978)

Measurements of the low-field ac susceptibility on ternary alloys of Pd+0.35 at.% Fe and a Mn concentration of 0 to 8 at.% reveal, for three distinct regimes of Mn concentration, (a) a giant-moment ferromagnetism, (b) a high-temperature ferromagnetic phase followed by a lower-temperature spin-glass transition, and (c) a spin-glass phase. Our results for the susceptibility and the  $T$ - $c$  phase diagram are satisfactorily explained by the spin-glass theory of Sherrington and Kirkpatrick.

Competing interactions in magnetic systems lead to a diversity of magnetic structures and critical phenomena. Particularly in insulating compounds, variations of the space and the spin dimensionalities provide important criteria for the theory of phase transitions. In metallic systems, and especially dilute alloys, the situation is more complex because of the long-range nature of the magnetic interactions mediated by the conduction electrons. If we focus upon dilute magnetic alloys and neglect the Kondo effect which produces a weakened magnetic moment, there exist two distinct types of ordering for randomly distributed magnetic impurities. The first is the so-called "giant-moment" ferromagnetism<sup>1</sup> which occurs in a few systems with a large exchange-enhanced host susceptibility. Secondly, there is the more common spin-glass type<sup>2</sup> of random freezing of the moments without long-range order in the usual sense.

An interesting combination of these two types of ordering is found at different concentrations of the PdMn system. For  $c \leq 3$  at.% Mn, giant-moment ( $\mu_{\text{eff}} \approx 7.5\mu_B$ ) ferromagnetism prevails.<sup>3</sup> However, upon further increasing the Mn concentration ( $c \geq 4$  at.%), the probability of having two

Mn atoms at first, second, and third nearest neighbor increases. This then supplies the essential element of "conflict" or "frustration" for the appearance of the spin-glass phase. Mn nearest neighbors couple antiparallel and thereby produce Mn-Mn antiferromagnetic exchange competing with the longer-ranged ferromagnetic interaction.<sup>4</sup> An anomalous mixed phase with peculiar magnetization and remanence behavior occurs between 3 and 4 at.% Mn.<sup>5</sup>

In order to better control and understand the competition between these two exchange mechanisms, we have studied the ternary alloy Pd + 0.35 at.% Fe and a Mn concentration of  $0 \leq c \leq 8$  at.%. PdFe is a strong giant-moment ferromagnet with  $\mu_{\text{eff}} \approx 10\mu_B$  and  $T_c = 8.7$  K for 0.35 at.% Fe. Only at very low concentrations ( $\approx 0.015$  at.% Fe) and temperatures ( $\approx 0.1$  K) is there some experimental evidence for the onset of a spin-glass ordering.<sup>6</sup> By adding Mn to this PdFe alloy we now have a wide Mn concentration range at favorable temperatures (1–20 K) with which to investigate the resulting magnetic ordering. Low-field susceptibility measurements offer a convenient and sensitive method to determine the type of magnetism present, and an external

magnetic field may be separately applied to obtain the field dependence of the differential susceptibility. A striking feature of our results for  $3 \leq c_{\text{Mn}} \leq 6$  at.% is the high-temperature ferromagnetism giving way to the spin-glass ordering at low temperatures.<sup>7</sup> In addition, the external field clearly increases  $T_c$  while shifting the spin-glass freezing temperature,  $T_f$ , to lower values.

A solvable model of a spin-glass has been presented by Sherrington and Kirkpatrick.<sup>8</sup> In this theory the spins are coupled by infinite-ranged, random interactions independently distributed with the Gaussian probability density

$$P(J_{ij}) = [2\pi J^2]^{-1/2} \exp[-(J_{ij} - J_0)^2/2J^2].$$

The  $J_0$  displacement from zero is essentially a ferromagnetic exchange coupling, and the distribution width,  $J$ , is a measure of the spin-glass interaction and  $T_f$ . Thus, depending upon the ratio of the intensive parameters  $\tilde{J}_0/\tilde{J}$  ( $\tilde{J}_0 = NJ_0$  and  $\tilde{J} = N^{1/2}J$  where  $N$  is the number of spins), both ferromagnetic and spin-glass phases can occur. The application and extension of this theory to our *Pd*FeMn measurements not only allows us to calculate with good agreement the susceptibility in the three distinct concentration regimes, but also results in a consistent phase diagram along with an indication of the external-field behavior.

The alloy samples were prepared by repeated induction melting in an Ar-gas atmosphere. First a large *Pd*+0.35-at.%-Fe master alloy was made and then the desired amount of Mn was added to pieces of the master alloy. A chemical analysis on each sample determined both the Fe and Mn concentrations. In order to insure alloy homogeneity, a heat treatment of 48 h at 1000°C was employed. Finally, we formed our alloys into perfect spheres with a spark-erosion technique. The susceptibility was measured via a standard mutual-induction bridge operating at a frequency of 210 Hz and a driving field of about 0.1 Oe. The temperature was controllable to within a few millikelvin between 1 and 20 K. A superconducting solenoid produced the external magnetic fields (up to ~1 kOe) which were parallel to the ac driving field.

In Fig. 1 we show the temperature dependence of the susceptibility in zero external field for Mn concentrations which typify the behavior in the three different  $c$  regimes. Curve *a* exhibits the sharp kneelike characteristic of a ferromagnet:  $\chi(\text{real}) = \chi(\text{measured})/[1 - D\chi(\text{measured})]$ , at  $T = T_c$ ,  $\chi(\text{real}) \rightarrow \infty$  and  $\chi(\text{measured}) = 1/D$ , where

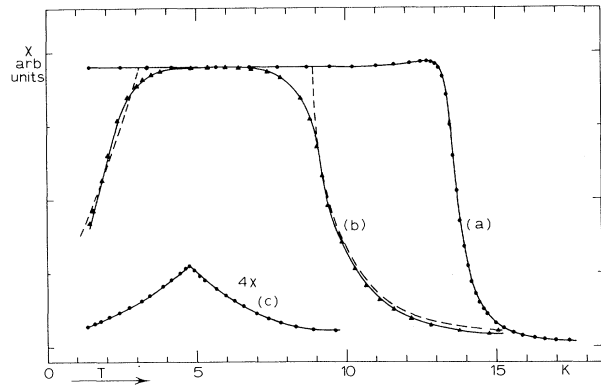


FIG. 1. Temperature dependence of the low-field (0.1 Oe) susceptibility for  $(\text{Pd}_{0.9965}\text{Fe}_{0.0035})_{1-x}\text{Mn}_x$ . Curve *a*,  $x = 0.01$ ; curve *b*,  $x = 0.05$ ; curve *c*,  $x = 0.065$ . The dashed curve represents the calculated susceptibility (see text).

$D$  is the demagnetization factor equal to 4.18 for a sphere. Because of the rounding of the transition,  $T_c$  is taken to be the temperature where  $d\chi/dT$  has its maximum value. A similar type of transition is also found in curve *b* at about 9 K. Note that there is more smearing in  $\chi(T)$ , but the same maximum value of  $\chi = 1/D$  is reached. This signifies a ferromagnetic transition. However, as the temperature is lowered to 5 K, the susceptibility dramatically decreases from the  $1/D$  ferromagnetic value. We interpret this strong reduction in  $\chi$  at low temperatures as due to a loss in response in  $M/H_{ac}$  signaling the onset of the random (no net moment) spin-glass state. A decreasing  $\chi$  with decreasing  $T$  epitomizes spin-glass freezing, and the reversed knee in  $\chi(T)$  determines  $T_f$ . For a larger Mn concentration, curve *c*, we have the full spin-glass  $\chi(T)$  characterized by the sharp peak or cusp at  $T_f$ .<sup>2</sup>

These  $T_c$  and  $T_f$  data may be collected for all twelve measured concentrations into a  $T$ - $c$  diagram with  $H = 0$  as is given in Fig. 2. The initial  $T_c$ - $c$  rise, maximum in  $T_c$ , and falloff above 2 at.% Mn is describable in terms of a simple model. Extension of the giant-moment theory of Takahashi and Shimizu<sup>9</sup> to our ternary alloys gives a transition temperature  $T_c = C_1 c_{\text{Mn}} + C_2 c_{\text{Fe}}$ , where  $C_1$  and  $C_2$  are constants equal to those for the respective binary *Pd*Mn and *Pd*Fe alloys. Thus  $T_c$  for *Pd*FeMn is given simply by a linear combination of the Fe and Mn concentrations. The initial slope of 5 K/at.% Mn in Fig. 2 is in fair agreement with the value 4 K/at.% Mn for the binary *Pd*Mn system.<sup>1</sup>

At larger concentrations we must take into ac-

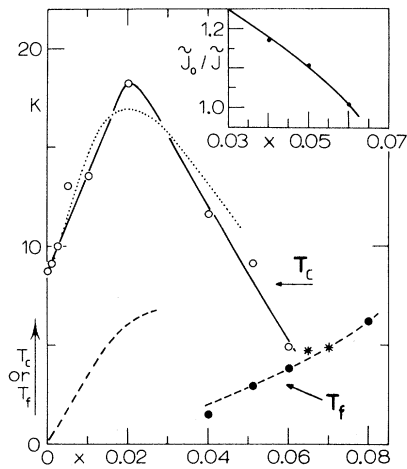


FIG. 2.  $T$ - $x$  diagram for  $(\text{Pd}_{0.9965}\text{Fe}_{0.0035})_{1-x}\text{Mn}_x$ . Ferromagnetic transitions are indicated by open circles; spin-glass transitions by closed circles; and intermediate, field-separable, transitions by asterisks. The dotted line represents our calculation of  $T_c$  and the dashed line is the phase diagram for binary  $\text{PdMn}$ . The inset shows the concentration dependence of  $\tilde{J}_0/\tilde{J}$  (see text).

count the direct antiferromagnetic Mn-Mn and Mn-Fe interactions.<sup>4,10</sup> We assume this interaction to be effective for all impurities within three-nearest-neighbor shells.<sup>4</sup> Thus, the ferromagnetism is determined by the interaction of those impurities four or more shells away from each other. Setting  $T_c$  proportional to the total concentration of impurity times the probability of having the first-three-neighbor shells fully occupied by Pd, we have approximately  $T_c = Ac_{\text{tot}}(1 - c_{\text{tot}})^{42}$ . The power 42 arises from the 12 + 6 + 24 sites in the first three shells of an fcc lattice. A reasonable agreement with the experimental data in Fig. 2 (see dotted curve) is obtained between 0 and 5 at.% Mn with  $A = 1960$  K.

Upon further increasing the Mn concentration the spin-glass phase clearly appears at lower temperatures ( $T_f < T_c$ ). This double transition (paramagnetic  $\rightarrow$  ferromagnetic  $\rightarrow$  spin-glass) at fixed concentration represents regime- $b$  susceptibility behavior. Finally, at yet higher concentrations ( $c > 6$  at.% Mn and  $H = 0$ ), the "pure" spin-glass state emerges with exactly the same  $T_f(c)$  dependence as the binary  $\text{PdMn}$  system<sup>11</sup>—see dashed lines in Fig. 2. Additional evidence for the double transition comes from the application of an external field. With  $H = 200$  Oe the  $\chi(T)$  peak for the intermediate 6.5- and 7-at.%-Mn samples (asterisks in Fig. 2) splits into a positive-temperature-shifted ferromagnetic bump<sup>12</sup> and a negative- $T$ -shifted drop similar to concen-

tration-regime- $b$   $\chi(T)$ . An analogous displacement of  $T_c$  to higher temperatures and  $T_f$  to lower also occurs in 4–6-at.%-Mn concentrations when a small (a few hundred oersteds) external field is applied. A reasonable explanation of this effect is that an external field is favorable for ferromagnetism, enhancing  $T_c$ ; in contrast, the field not only smears the spin-glass transition<sup>2</sup> but hinders its occurrence. Such susceptibility studies in an external field open up a new dimension in the  $T$ - $c$  phase diagram and more diversified critical phenomena. Our extensive  $\chi(T, H)$  measurements will be published in a subsequent paper.

The problem of mixed ferromagnetic and anti-ferromagnetic exchange has been treated by Sherrington and Kirkpatrick<sup>8</sup> (SK). In particular, these authors explore the competition of a long-range ferromagnetic order with the spin-glass phase. From their free energy<sup>13</sup>  $F$ , the susceptibility may be calculated as  $\chi = -\partial^2 F / \partial H^2$  in terms of the two parameters  $\tilde{J}_0$  and  $\tilde{J}$ , the strengths of the ferromagnetic and spin-glass interactions, respectively. The resulting simple relation for  $\chi$  in terms of  $\chi(\tilde{J}_0 = 0)$  is

$$\chi(T) = \chi(\tilde{J}_0 = 0) / [1 - \tilde{J}_0 \chi(\tilde{J}_0 = 0)].$$

In order to compare the calculated susceptibility with the measured one for the ferromagnetic case, demagnetization effects must again be taken into account. In Fig. 1 the dashed line represents the result of this calculation for  $\tilde{J}_0/\tilde{J} = 1.1$  with  $\tilde{J} = 8.1k_B$ , the ferromagnetic-spin-glass case (curve  $b$ ). The excellent agreement with the experimental data for 5 at.% Mn is evident and thereby emphasizes our interpretation in terms of a double transition.

The phase diagram, calculated by SK (Fig. 1 of Ref. 8), contains the essential properties of ours. For values of  $\tilde{J}_0/\tilde{J}$  between 1.00 and 1.25 a paramagnetic  $\rightarrow$  ferromagnetic  $\rightarrow$  spin-glass transition may occur. By equating our measured value of  $T_c/T_f$  at fixed concentration to the same ratio from the SK phase diagram, the value of  $\tilde{J}_0/\tilde{J}$  may be determined for this concentration. The inset in Fig. 2 shows the  $\tilde{J}_0/\tilde{J}$  vs  $c$  behavior. Therefore, it can be concluded that for  $c > 6$  at.% Mn only paramagnetic to spin-glass transitions are possible since  $\tilde{J}_0/\tilde{J} < 1$ , and for  $c < 3$  at.% Mn only paramagnetic to ferromagnetic transitions are allowed since  $\tilde{J}_0/\tilde{J} > 1.25$ . The mixed regime lies between these two limits.

In summary, we have measured the low-field

susceptibility for a series of ternary  $PdFeMn$  alloys with varying Mn concentration. Three distinct concentration regimes are determined which correspond to a giant-moment ferromagnet, a double or mixed transition (paramagnetic  $\rightarrow$  ferromagnetic  $\rightarrow$  spin-glass), and a spin-glass. Both the susceptibility experiments and the phase diagram are interpretable in terms of the model of Sherrington and Kirkpatrick. An external magnetic field enhances the ferromagnetism while hindering the formation of the spin-glass phase. This opposite shifting of  $T_c(H)$  and  $T_f(H)$  leads to an interesting variety of critical and multicritical phenomena.

This work was supported by the Stichting voor Fundamenteel Onderzoek der Materie (FOM-TNO). We wish to acknowledge stimulating discussions with K. H. Bennemann and to thank the crystal and chemical departments of the Kamerlingh Onnes Laboratorium for their assistance with the sample preparation and analysis.

<sup>1</sup>For a review see G. J. Nieuwenhuys, *Adv. Phys.* **24**, 515 (1975).

<sup>2</sup>For reviews see J. A. Mydosh, in *Magnetism and*

*Magnetic Materials-1974*, AIP Conference Proceedings No. 24, edited by C. D. Graham, Jr., G. H. Lander, and J. J. Rhyne (American Institute of Physics, New York, 1976), p. 131; K. H. Fischer, *Physica (Utrecht)* **86-88B**, 813 (1977).

<sup>3</sup>W. M. Star, S. Foner, and E. J. McNiff, Jr., *Phys. Rev. B* **12**, 2690 (1975).

<sup>4</sup>G. J. Nieuwenhuys and B. H. Verbeek, *J. Phys. F* **7**, 1497 (1977).

<sup>5</sup>C. N. Guy and W. Howarth, in *Amorphous Magnetism II*, edited by R. A. Levy and R. Hasegawa (Plenum, New York, 1977), p. 169.

<sup>6</sup>K. Nagamine, N. Nishida, S. Nagamiya, O. Hashimoto, and T. Yamazaki, *Phys. Rev. Lett.* **38**, 99 (1977).

<sup>7</sup>Evidence for a similar type of behavior (ferromagnetism to mictomagnetism) has recently been found in the FeAl system by R. D. Shull, H. Okamoto, and P. A. Beck, *Solid State Commun.* **20**, 863 (1976). See also J. W. Cable, L. David, and R. Parra, *Phys. Rev. B* **16**, 1132 (1977).

<sup>8</sup>D. Sherrington and S. Kirkpatrick, *Phys. Rev. Lett.* **35**, 1792 (1975).

<sup>9</sup>T. Takahashi and M. Shimizu, *J. Phys. Soc. Jpn.* **20**, 26 (1965), and **23**, 945 (1967).

<sup>10</sup>T. Moriya, *Prog. Theor. Phys.* **34**, 329 (1965).

<sup>11</sup>H. A. Zweers, W. Pelt, G. J. Nieuwenhuys, and J. A. Mydosh, *Physica (Utrecht)* **86-88B**, 837 (1977).

<sup>12</sup>I. Maartense and G. Williams, *J. Phys. F* **6**, L121, 2263 (1976).

<sup>13</sup>See also K. H. Fischer, *Solid State Commun.* **18**, 1515 (1976).

## Time-Dependent Ginzburg-Landau Model of the Spin-Glass Phase

Shang-keng Ma

*Department of Physics and Institute for Pure and Applied Physical Sciences, University of California, San Diego, La Jolla, California 92093*

and

Joseph Rudnick<sup>(a)</sup>

*IBM Thomas J. Watson Research Center, Yorktown Heights, New York 10598*

(Received 12 August 1977)

The Edwards-Anderson spin-glass phase is studied via time-dependent Ginzburg-Landau models with quenched impurities. A perturbation expansion is used to study the dynamics and statics without the use of the replica method. It is shown that the spin correlation function has a  $t^{-1/2}$  long-time tail in the spin-glass phase.

The Edwards-Anderson spin-glass phase, characterized by a frozen magnetization with zero spatial average, has received much recent attention.<sup>1-7</sup> Most of the analytical studies have been on the static properties using the replica ( $n \rightarrow 0$ ) method. In this Letter we report results on both the dynamics and statics of certain time-dependent Ginzburg-Landau (TDGL) models which exhibit a spin-glass phase. We make no use of the replica method. In fact, it is our purpose to avoid the replica method, which is in several ways artificial and conceals the basic physics. This simple analysis, using TDGL models, is complementary to the numerical Monte Carlo work and to other methods reported recently.<sup>4,5</sup>

Our models are defined by the following equation of motion for an  $n$ -component vector spin density